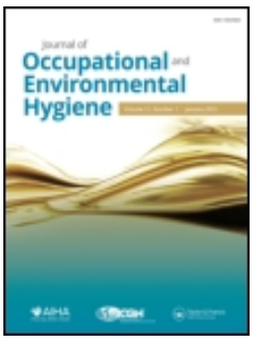

Taylor & Francis
Taylor & Francis Group

Journal of Occupational and Environmental Hygiene

ISSN: 1545-9624 (Print) 1545-9632 (Online) Journal homepage: http://www.tandfonline.com/loi/uoeh20

Study of contact characteristics between a respirator and a headform

Mang Cai, Shengnan Shen, Hui Li, Xiaotie Zhang & Yanzhao Ma

To cite this article: Mang Cai, Shengnan Shen, Hui Li, Xiaotie Zhang & Yanzhao Ma (2016) Study of contact characteristics between a respirator and a headform, Journal of Occupational and Environmental Hygiene, 13:3, D50-D60, DOI: 10.1080/15459624.2015.1116699

To link to this article: http://dx.doi.org/10.1080/15459624.2015.1116699

Accepted author version posted online: 11 Nov 2015.
Published online: 28 Jan 2016.

JOURNAL OF OCCUPATIONAL AND ENVIRONMENTAL HYGIENE
2016, VOL. 13, NO. 3, D50–D60
http://dx.doi.org/10.1080/15459624.2015.1116699

Taylor & Francis
Taylor & Francis Group

Case Study
Column Editor: James Couch

Study of contact characteristics between a respirator and a headform

Reported By
Mang Cai, Shengnan Shen, Hui Li, Xiaotie Zhang, and Yanzhao Ma

School of Power and Mechanical Engineering, Wuhan University, Wuhan, China

ABSTRACT

This article presents a computational study on contact characteristics of contact pressure and resultant deformation between an N95 filtering facepiece respirator and a newly developed digital headform. The geometry of the headform model is obtained based on computed tomography scanning of a volunteer. The segmentation and reconstruction of the headform model is performed by Mimics v16.0 (Materialise, Leuven, Belgium), which is a medical image processing software. The respirator model is obtained by scanning the surface of a 3M 8210 N95 respirator using a 3D digitizer and then the model is transformed by Geomagic Studio v12.0 (3D system, Rock Hill, SC), a reverse engineering software. The headform model contains a soft tissue layer, a skull layer, and a separate nose. The respirator model contains two layers (an inner face sealing layer and an outer layer) and a nose clip. Both the headform and respirator are modeled as solid elements and are deformable. The commercial software, LS-DYNA (LSTC, Livermore, CA), is used to simulate the contact between the respirator and headform. Contact pressures and resultant deformation of the headform are investigated. Effects of respirator stiffness on contact characteristics are also studied. A Matlab (MathWorks, Natick, MA) program is developed to calculate local gaps between the headform and respirator in the stable wearing state.

KEYWORDS
CT scanning; digital headform; finite element method; fit and comfort; respirator

Introduction

With rapid economic growth over the past several decades, China's extensive industrial development, substantial coal-dependent energy consumption, and increasing number of vehicles have led to a rise in air pollutants emissions. Air pollution has serious direct effects on public health in China. Studies on the effects of air pollution on health showed that between 350,000 and 500,000 people die prematurely each year as a result of outdoor air pollution in China.[1–4] Air pollutants contain large number of harmful chemical substances (SO_2, NO_x) and fine suspended particular matter. Yang et al.[5] reported that particulate matter with an aerodynamic diameter of less than 2.5 μm ($PM_{2.5}$) has become the fourth biggest threat to the health of the Chinese people. In daily life, a common way to prevent the inhalation of air pollutants especially $PM_{2.5}$ is to wear a respirator. The most commonly used respirator is N95 respirator, which belongs to the N series and filters at least 95% of airborne particles. Respirator comfort and fit are two important parameters for respirator design, usage, and standard development. Numerous factors such as strap forces, facial features, seal material, respirator size, and respirator shape are most likely to affect respirator comfort and fit. This article attempts to conduct a computational study on contact pressure and facial deformation between an N95 filtering facepiece respirator (FFR) and a headform. The goal is to obtain better respirator fit and comfort.

For the past few decades, significant research has been done in terms of both experimental and simulation approaches for respirator comfort and fit. Earlier research on respirator comfort and fit were mainly based on experimental tests. Snook et al.[6] investigated the force that a respirator facepiece exerts against the face as a factor in respirator discomfort. Their work concluded that facial locations differ in sensitivity to force, but these differences are not significant enough to cause any major changes in

CONTACT Shengnan Shen 00030684@whu.edu.cn School of Power and Mechanical Engineering, Wuhan University, Wuhan, China 430072.
Color versions of one or more of the figures in the article can be found online at www.tandfonline.com/uoeh.

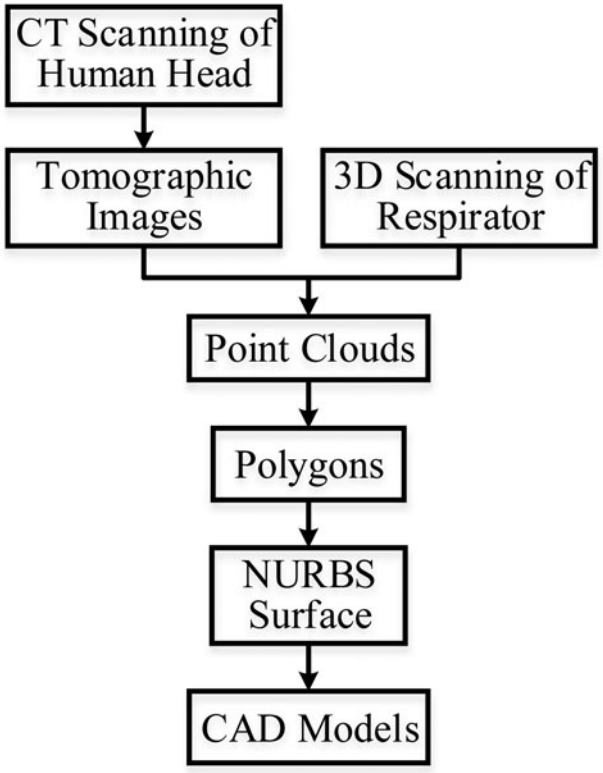

Figure 1. Procedure of generating the headform and respirator models.

respirator design. Manninen et al.[7] studied face seal leakages and the comfort in the use of six kinds of respiratory protective devices used in agricultural work under laboratory and field conditions. The face seal leakages of these devices were measured and volunteers were interviewed about their subjective opinions on the use of the devices. Akbar-Khanzadeh et al.[8] investigated the degree of comfort of personal protective equipment (PPE) in an automobile encapsulating plant. Their work suggested that to increase the effectiveness and safety of PPE, the human-factor aspects of PPE design should be emphasized more and quality improvement should cover the wearability of PPE. Cohen[9] proposed an experimental method for evaluating mask seals by measuring seal pressure distributions and developed a relationship between fit factor and sealing pressure distributions for evaluating the sealing performance. Zhuang et al.[10] investigated the effects of subject characteristics (gender and face dimensions) and respirator features on respirator fit. Later, Zhuang et al.[11] investigated the correlation between respirator fit and the new NIOSH respirator fit test panel cells for various respirator sizes.

Despite valuable information are provided by experimental data, these approaches are time consuming and expensive. The experimental measures may have large errors due to the limitation of the laboratory equipment.

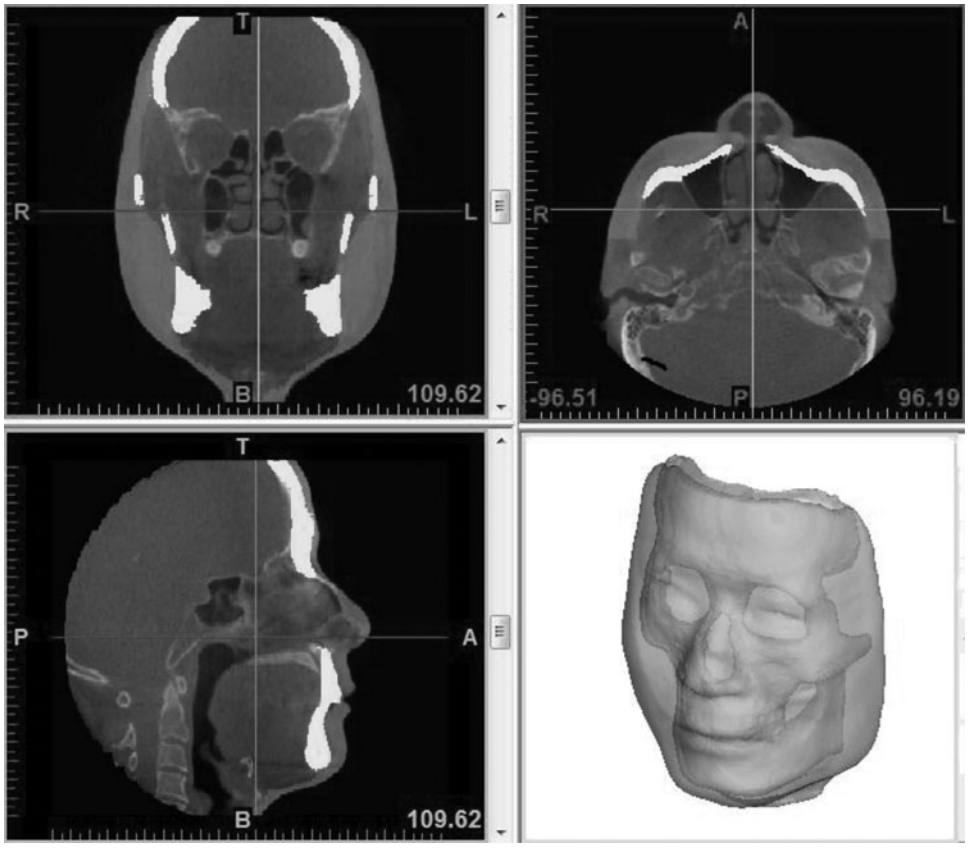

Figure 2. Human head segmented from CT data by Mimics.

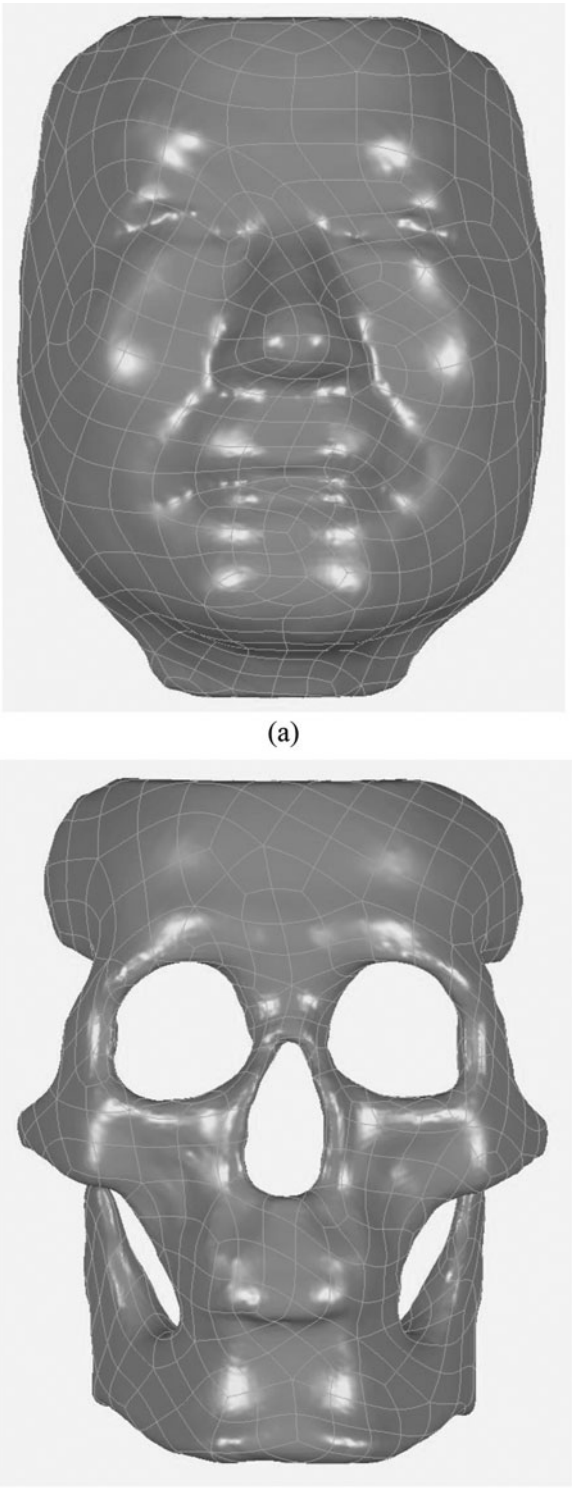

Figure 3. CAD models of the headform: (a) soft tissue and (b) skull.

A lack of reproducibility and stability caused by human factor as well as individual subject may also lead to large errors. On the other hand, with rapid increases in computational technology, numerical simulations using finite element (FE) method offer a time-saving, cost-effective, and reproducible alternative to experimental methods. Bitterman[12] performed FE simulation between a simplified pilot face model and an oxygen mask model and calculated contact pressure between them. Piccione et al.[13] modeled the interface between the respirator and headform and evaluated respirator fit and discomfort using DYNA3d, which is an explicit 3D code and an older version of LS-DYNA (LSTC, Livermore, CA). Zhuang et al.[14] developed five different sizes of digital 3D headforms that represent facial features of the current U.S. work force. These headforms could be incorporated into respirator research, certification standards and design. Yang et al.[15] used FE software LS-DYNA (LSTC, Livermore, CA) to simulate the interaction between a respirator and a medium-sized headform model developed by Zhuang et al.[14] Contact pressures on both the respirator and headform during the interaction process with different strap forces were analyzed. Later, Dai et al.[16] investigated parameters such as strap tension, strap orientation, strap location, friction coefficient, and seal material stiffness affecting contact pressure between a respirator and the same medium-sized headform model developed by Zhuang et al.[14] Lei et al.[17] simulated contact pressure between six N95 FFRs and five digital headform models developed by Zhuang et al.[14] and validated their results through experiments. In their study, the headform model was divided into five parts with multiple layers. However, all the layers of the five parts were not continuous. Slip occurred between each layer, which was not consistent with real structure of human head. In China, Yu et al.[18] also developed five digital 3D headforms representative of Chinese workers. The headforms they developed contain only one layer, the same as developed by Zhuang et al.[14] These earlier FE studies had provided some insights into respirator comfort and fit. Nonetheless, they had made some assumptions and simplifications in the geometry of the headform. More recently, Yang et al.[19] developed a high-quality human headform with detailed information of soft tissues and intracranial components based on computed tomography (CT) and magnetic resonance imaging (MRI). But there is still no research that uses models created by CT scanning or MRI to study contact characteristics between a respirator and headform.

The objective of this study is to investigate the contact characteristics during wearing a respirator on a headform. Three-dimensional geometric models of a typical Chinese headform and a 3M 8210 $PM_{2.5}$ respirator are developed by using CT scanning method and 3D scanning method, respectively. Corresponding FE models are generated using software HyperMesh v12.0 (Altair HyperWorks, Troy, MI). Then, the wearing process of the respirator on the headform is studied by

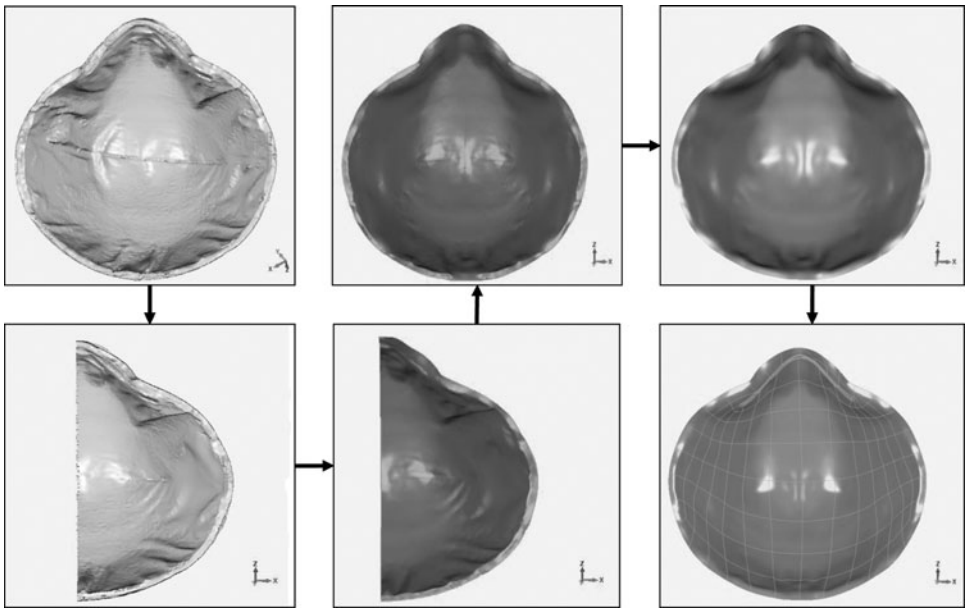

Figure 4. Six steps to develop the CAD model of the respirator.

performing contact simulation using software LS-DYNA (LSTC, Livermore, CA). The contact pressure, headform deformation, and resultant gaps between the headform and respirator are simulated. Also, the effects of the stiffness of respirator inner layer on contact characteristics are investigated.

Simulation models and methods

Geometric models

The procedure of geometric models generation is shown in Figure 1.

Headform model

An X-ray CT scanner is used to get tomographic images of a Chinese male (175 cm/70 kg). The resolution/thickness of the CT is 0.42/1.0 mm. It can get internal layer-structures of the headform so that the models will be more accurate than that obtained by a 3D scanning which can only get surface features of the headform. First, tomographic images of the headform are obtained by CT scanning. Second, the CT scanned images of the headform model are imported into Mimics v16.0 (Materialise, Leuven, Belgium) to reconstruct the skull layer and the soft tissue layer by segmentation. The skull layer and the soft tissue layer are separated by using Boolean operations. Once separated, both layers are visualized in 3D and a file is created in the form of STL. Third, the STL file is imported into Geomagic Studio v12.0 (3D system, Rock Hill, SC), a reverse engineering software which can transfer triangular surfaces to Non-Uniform Rational B-spline (NURBS) models and CAD models. Fourth, a NURBS surface is created by applying a surface over its underlying polygons. Finally, the CAD model is obtained by converting the NURBS surface. CT imaging and three dimensional visualizations of the headform are shown in Figure 2. CAD models of the headform are shown in Figure 3.

Respirator model

A PowerScan 3D digitizer (Power3D, Wuhan, China) is used to get original data of a 3M 8210 N95 respirator. The procedure of generating the respirator model is similar to that of the headform model with a few differences which is shown in Figure 1. Figure 4 shows six steps to develop the CAD model of the respirator. First, a 3M 8210 $PM_{2.5}$ respirator is scanned by a PowerScan-IIS 3D digitizer (Power3D, Wuhan, China) to form the point cloud model and a STL file is created. Second, the file is imported into Geomagic Studio v12.0 (3D system, Rock Hill, SC). Note that the original coordinate system of the point cloud model is not consistent with the world coordinate system in the software, which will make it difficult to align the respirator model with the headform model in the contact simulation. Therefore, it is necessary to transform the original coordinate system of model to coincide with the world coordinate system. After transformation, point clouds are wrapped into polygons. To reduce the non-symmetry error caused by the scanning, the polygon model is trimmed by a symmetry plane and a half of the polygon model is obtained. Then, it is mirrored to create a complete model of the respirator. After that, a NURBS surface is created by applying a surface over its underlying polygons. Finally, the CAD model is obtained by converting the NURBS surface.

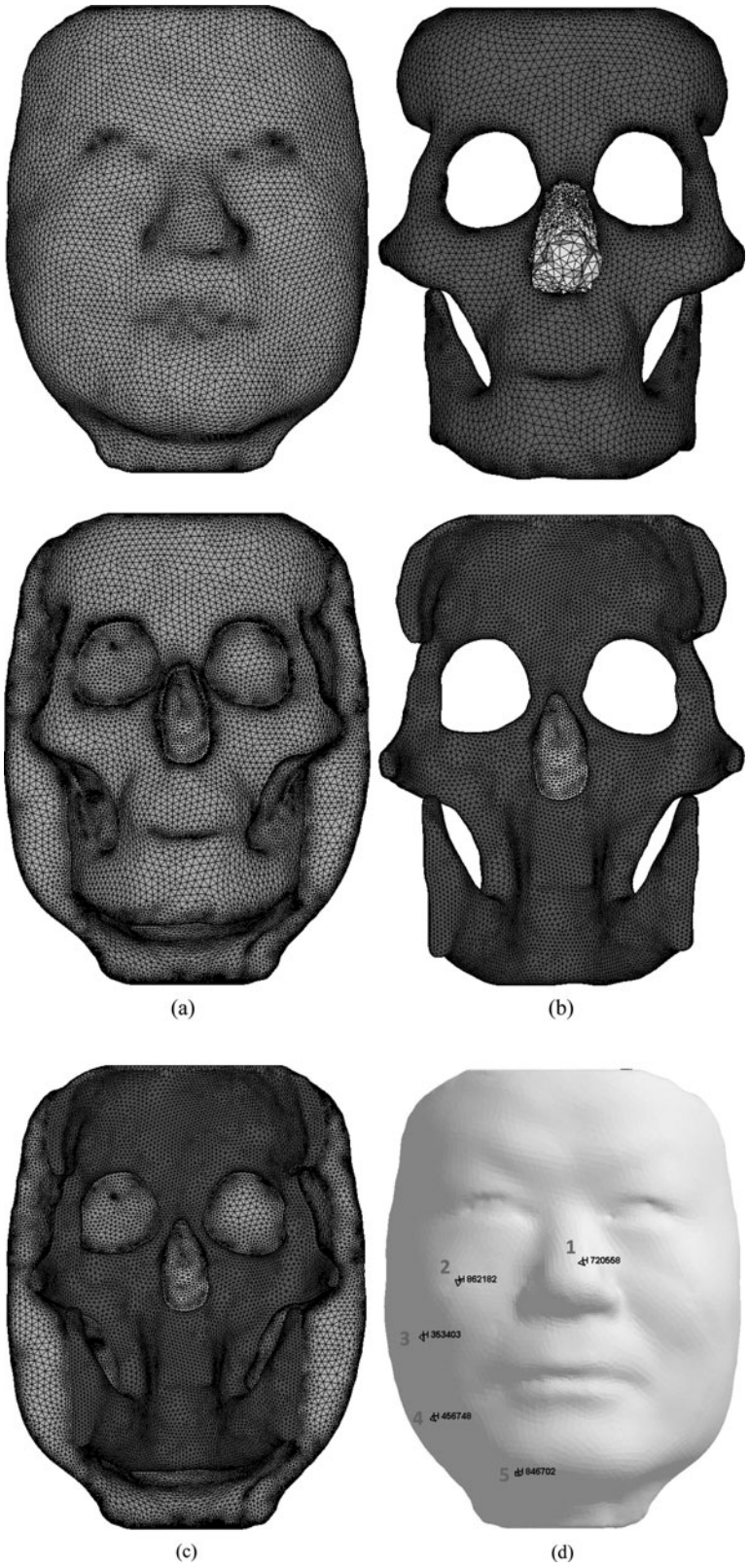

Figure 5. FE models of the headform: (a) soft tissue, (b) skull, (c) two parts together, and (d) five interesting elements.

Figure 6. FE model of the respirator.

Simulation methods

HyperMesh v12.0 (Altair HyperWorks, Troy, MI) is used to generate the FE meshing of both the headform and respirator models. The mechanical properties of the meshed models and simulation conditions are defined in LS-PREPOST, pre- and post-processor of LS-DYNA (LSTC, Livermore, CA).

The CAD model of the headform has a very complex shape and contains many curved sub-surfaces. A semi-automatic meshing technique is employed in HyperMesh v12.0 (Altair HyperWorks, Troy, MI) to mesh the headform model with an average element size of 3 mm and aspect ratio of 1. After importing the CAD model into HyperMesh v12.0 (Altair HyperWorks, Troy, MI), a set of 2D elements are created on the surface of the model. Then, all the 2D elements are tetrameshed into solid elements. The soft tissue is meshed into 245,611 tetrahedron solid elements while the skull is meshed into 157,651 elements for FE analyzing. The nose is separated from the soft tissue part and is composed of 19,760 tetrahedron solid elements. The headform mesh is shown in Figures 5a–c. Five elements on the left half of the headform are chosen to check the contact pressure values, as shown in Figure 5d.

The FE model of the respirator is designed to have an inner face sealing layer and an outer layer which is similar to that used by Lei et al.[17] In addition, a flexible nose clip is added on the basis of the two layers. After importing the CAD model into HyperMesh v12.0 (Altair HyperWorks, Troy, MI), the whole surface is meshed into triangle elements. Two layers of pentahedron solid elements are obtained by offsetting the 2D mesh. The nose clip is obtained by using the similar method. As shown in Figure 6, the inner layer of the respirator has a thickness of 1 mm, the outer layer has a thickness of 2 mm, and the nose clip has a thickness of 1 mm. The FE model of the respirator contains total 57,999 tetrahedron solid elements.

Mechanical properties

According to anatomy of human head, the human headform contains several layers, including skull, muscle, fatty tissue, and skin. [20] However, in this simulation only the skull layer, a combination of soft tissue layers, and the nose are modeled. The skull has mechanical properties of density of 4.5 g/cm^3, Young's modulus of 1000 MPa, and Poisson's ratio of 0.37.[21,22] We choose 1.4 g/cm^3 as the density of soft tissue to compensate for the assumption of one layer. Similarly, the Young's modulus is chosen as 0.7 MPa and Poisson's ratio is chosen as 0.45 for the soft tissue.[21,22] We simplify the nose as a whole part and assume it to have a density of 1.5 g/cm^3, Young's modulus of 30 MPa, and Poisson's ratio of 0.45.[23] For the FE model of the respirator, two layers are assigned as elastic materials while the nose clip is considered as plastic material. Mechanical properties of the two layers are the same as properties used by Lei et al.[17] The nose clip has mechanical properties close to that of malleable aluminum. Mechanical properties of both two FE models are listed in Table 1.[21–23]

Load and boundary conditions

Figure 7 shows the load conditions in this simulation. Force loads are applied on four corners of the respirator where straps are attached. Each corner contains 80 nodes. Load locations and force directions are illustrated

Table 1. Mechanical properties of FE models.

FE models	Components	Density (g/cm^3)	Young's modulus (MPa)	Poisson ratio
Headform	Soft tissue	1.4	0.7	0.45
	Skull	4.5	1000	0.37
	Nose	1.5	30	0.45
Respirator	Inner layer	1.39	27.7	0.37
	Outer layer	1.39	7	0.4

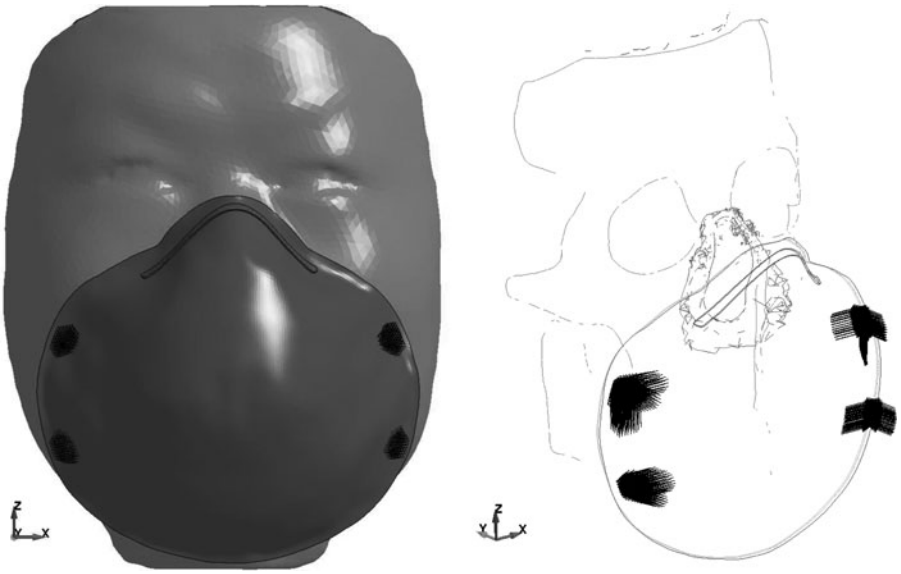

Figure 7. Load positions on the respirator.

in Table 2. The skull is treated as immovable and its back is constrained in all directions. After that, an automatic-surface-to-surface contact is defined. The surface of headform soft tissue is chosen as the master segment and the inner surface of the respirator is chosen as the slave segment. The contact simulation is performed by software LS-DYAN (LSTC, Livermore, CA). In the simulation, it focuses on contact characteristics between the headform and respirator. Thus, the nose clip is not artificially pressed towards the nose during the wearing process for simplification.

Simulation results

By performing contact simulation between the headform and respirator using the LS-DYNA (LSTC, Livermore, CA) explicit solver, the distribution of the contact pressure between the headform and respirator with time are shown in Figure 8. From Figure 8a, we observe that the upper cheek of headform starts to contact with the respirator at $t = 4$ ms. Then the contact area on the headform continues to spread widely with time, as well as the high pressure area. Concentrated pressures have already appeared at the cheek at $t = 20$ ms (Figure 8b). Figure 8c shows that the headform nearly contacts with the respirator completely. At last, the contact remains stable, as shown in Figure 8d. It is noted that there are no pressure distribution on both sides of the nasal bridge, since the nose clip is not artificially pressed towards nose in this work. Moreover, several areas exhibit high contact pressures: the nasal bridge, left chin, upper left cheek, middle left cheek, and lower left cheek. The highest pressure value is 0.11 MPa at the nasal bridge. This may be accounted for bony prominences of the skull. According to the previous study,[6] high pressures may make wearers feel discomfort, so it needs further improvement.

Table 2. Load conditions on the respirator.

	Load force (Newton)		
Load location	*X*-direction	*Y*-direction	*Z*-direction
Left/upper	−2	4	1
Right/upper	2	4	1
Left/Lower	−2	4	0
Right/Lower	2	4	0

Figure 9 shows the contour of the headform deformation induced by contact pressure during wearing process. Deformed areas increase with time. In the steady state (Figure 9d), the area of nasal bridge, and middle cheek exhibit large deformations, and the largest deformation is 0.93 mm at middle cheek. It should be noted that large deformation may cause facial discomfort.

By comparing Figure 8 with Figure 9, it is also found that areas on the headform with high contact pressures and large deformations during the wearing process are not exactly the same. Specially, the upper cheek and lower cheek have high pressures but their deformations are small.

According to the simulation results[17] and experimental results,[24] air leakages happen adjacent to areas that have high pressures, namely, an uneven distribution of pressure on the contact area cause air leakages. Thus, areas adjacent to the high contact pressure areas possibly happen air leakage. That is, areas adjacent to nasal bridge, upper cheek, and lower cheek could have air leakages.

Figure 10 shows profiles of contact pressure and deformation on five interesting elements. It can be seen in Figure 10a that the nasal bridge (element 1) exhibits

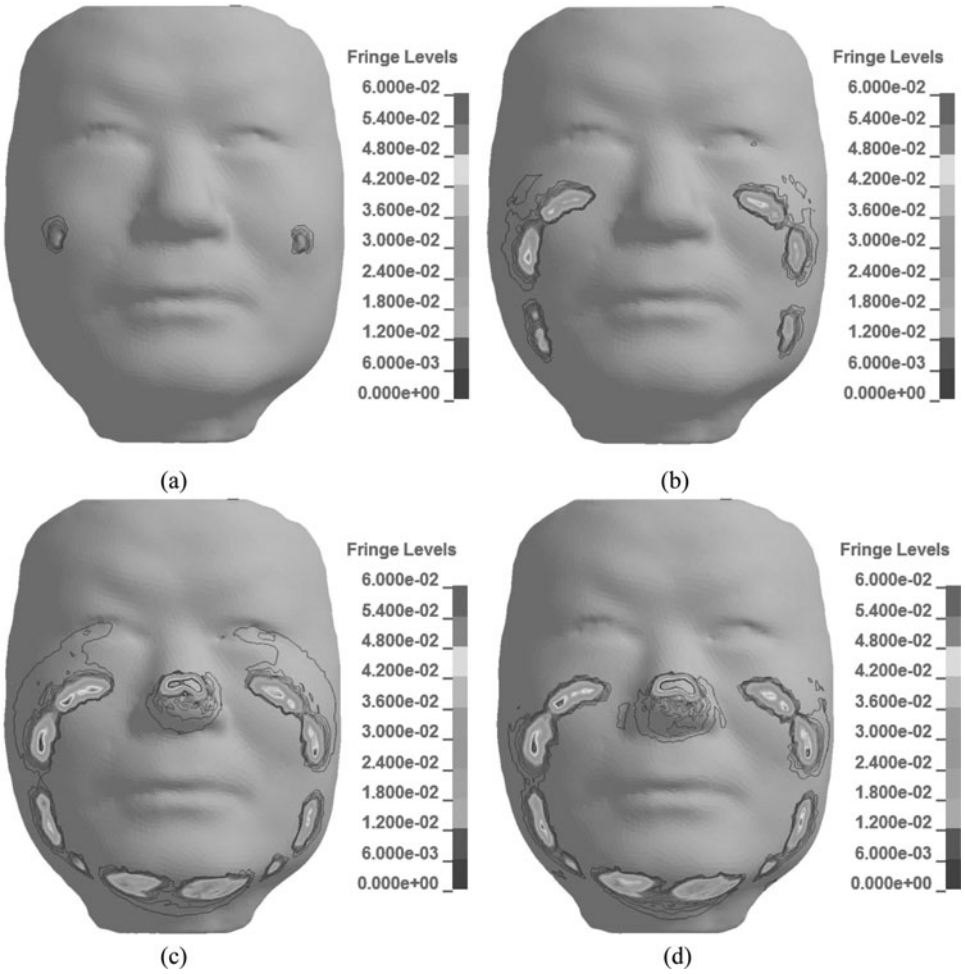

Figure 8. Contour of pressure distribution (unit: MPa) on the headform based on elements at time points of: (a) $t = 4$ ms, (b) $t = 20$ ms, (c) $t = 34$ ms, and (d) $t = 64$ ms.

the highest pressure, reaching 0.11 MPa. The middle cheek (element 3) has a pressure of 0.10 MPa while the upper cheek (element 2) and the lower cheek (element 4) exhibit smaller values, reaching 0.07 MPa and 0.08 MPa, respectively. The pressure on the chin (element 5) is 0.06 MPa, which is the smallest among five elements. From Figure 10b, it can be observed that the middle cheek (element 3) displays the largest deformation, reaching 0.93 mm. The nasal bridge (element 1) has a deformation of 0.87 mm. The upper cheek (element 2), lower cheek (element 4), and chin (element 5) exhibit lower values with 0.53 mm, 0.60, mm and 0.52 mm, respectively. It can be concluded that areas on the headform with high contact pressures and large deformation during the wearing process are not same, which are also verified in Figures 8 and 9.

Figure 11 shows five typical gaps between the headform and respirator in a stable wearing state. It is found that the local gap at different locations varies a lot due to the complex structure of the headform. The largest gap is 1.35 mm at the upper cheek (node B), and the smallest distance is 0.25 mm at the lower cheek (node D). Theoretically, a gap larger than zero means not sealed well there. Therefore, the upper cheek is more likely to have air leakage and an additional measurement should be taken to prevent it.

Figure 12 shows the pressure and resultant deformation of five interesting elements as a function of the respirator inner layer stiffness in a stable wearing state. From Figure 12a, we observe that contact pressures on the nasal bridge (element 1), upper cheek (element 2), and middle cheek (element 3) increase with the increase of the respirator's Young's modulus. However, the contact pressure on the lower cheek (element 4) suffers a reduction and it keeps almost unchanged on the chin (element 5). As the Young's modulus of the respirator increases from $0.4 \times E0$ to $2.0 \times E0$, the contact pressure increases by 66.3% on the nasal bridge (element 1), by 75.1% on the upper cheek (element 2), and by 44.5% on the middle cheek (element 3), while it decreases by 19.9% on the lower cheek.

Effects of respirator stiffness on resultant deformation are shown in Figure 12b. Simulation results show that as the Young's modulus of the respirator increases from

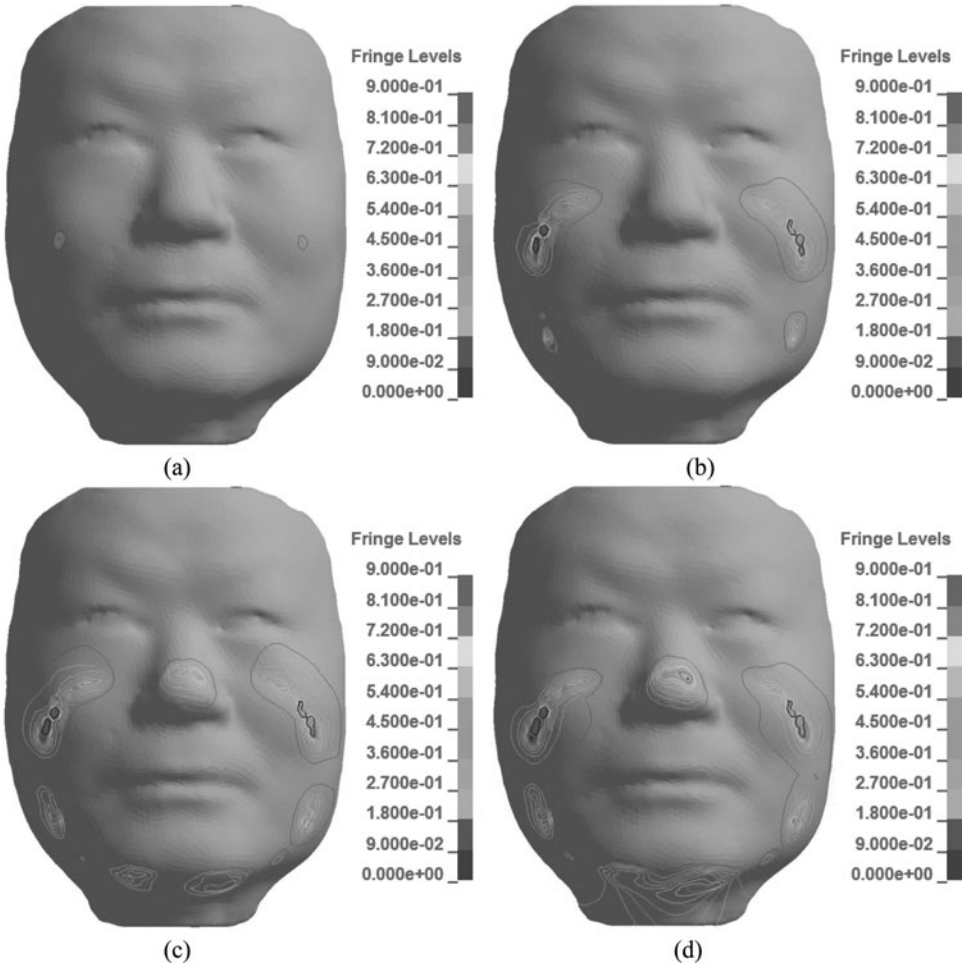

Figure 9. Contour of resultant deformation (unit: mm) of the headform based on nodes at time points of: (a) $t = 4$ ms, (b) $t = 20$ ms, (c) $t = 34$ ms, and (d) $t = 64$ ms.

$0.4\times$E0 to $2.0\times$E0, the resultant deformation of the nasal bridge (element 1), the upper cheek (element 2), and the chin (element 5) increases by 8.5%, 28.4%, and 8.8%, respectively. However, the resultant deformation of the lower cheek (element 4) suffers a reduction by 11.7% and it remains almost unchanged on the chin (element 5). From the results given above, it is found that the stiffness of the respirator inner layer affects the contact pressure as well as deformation greatly.

Discussion

This study used a respirator model and a headform model to study characteristics of the contact simulation. However, different sizes of headforms may affect pressure distribution and resultant deformation. For instance, Zhuang et al.[14] developed five different sizes of headforms that represent facial features of current U.S. work force. Yu et al.[18] also developed five digital 3D headforms representative of Chinese workers. Note that all the headforms in the two literatures were made up of only one layer. In addition, there are three types of respirators: one-size-fits-all, two size, and three size. Thus, there are many different contact combinations between the headform and respirator, which may have different results. Due to the low visibility of soft tissues in CT data, it obtains skull with high fidelity while the details of soft tissues are lost. In this study, soft tissues were obtained from CT scanning and were reconstructed as a whole part. The nasal bridge was also simplified for its complex structure. It should be highlighted that multiple scans of human head may do harm to the brain. On the other hand, MRI scanning can get details of soft tissues as well as that of nose while losing detailed information of skull. Thus, to develop a high-fidelity headform model including face skin, muscles, fatty tissue, skull, and nose, a combination of CT and MRI methods is needed. As an incomplete headform with only the front half part was used in the simulation, the straps of the respirator were not directly included in the simulation, but the strap forces were applied on four corners where the straps are attached. For simplicity in

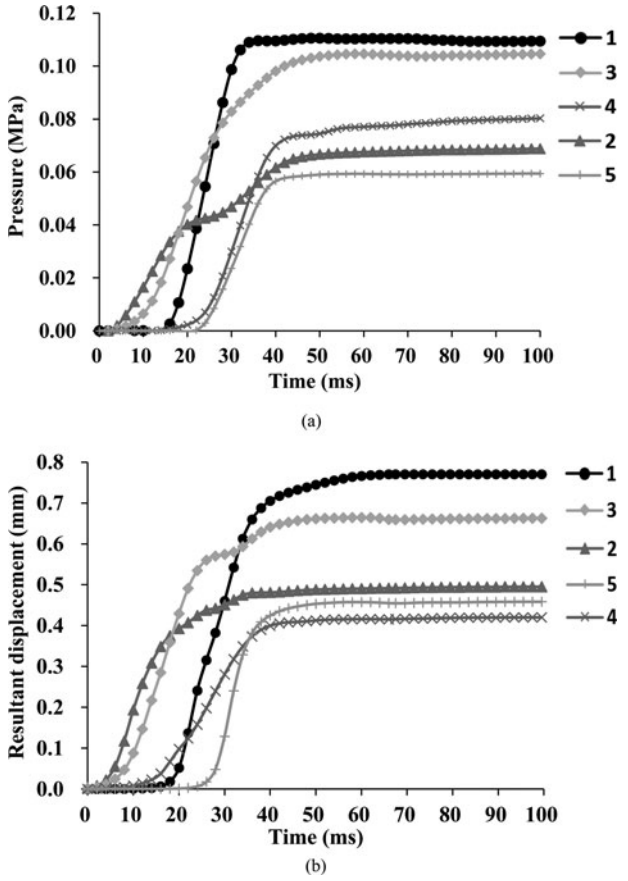

Figure 10. (a) Pressure profiles and (b) displacement profiles on five interesting elements.

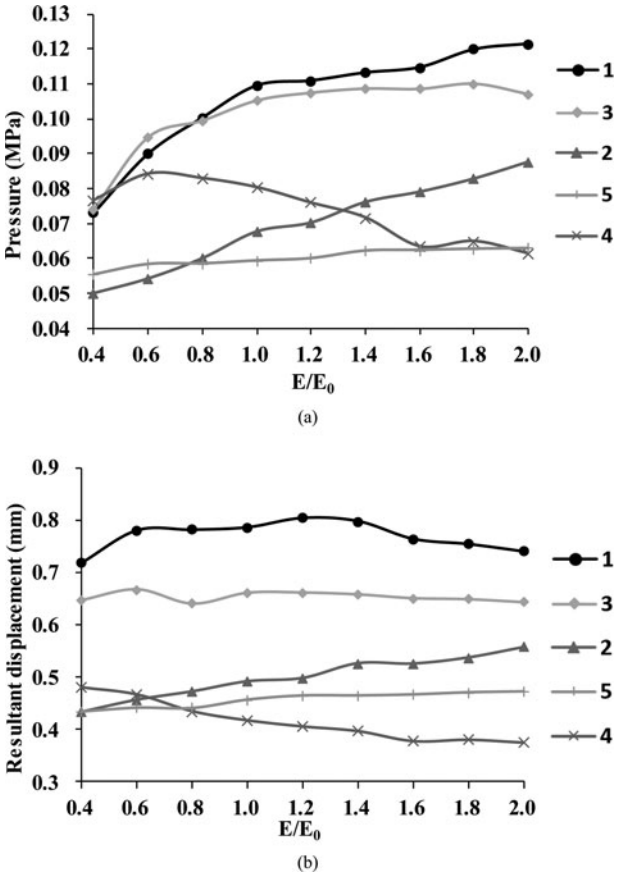

Figure 12. Pressure and resultant deformation on the five interesting elements as a function of stiffness of inner respirator layer (*E*: Young's modulus): (a) pressure profiles and (b) resultant displacement profiles.

the contact simulation, the nose clip was not artificially pressed tightly towards the nose after wearing the respirator.

Therefore, our future work will include:

(1) developing an entire and more biofidelic FE model of human head,

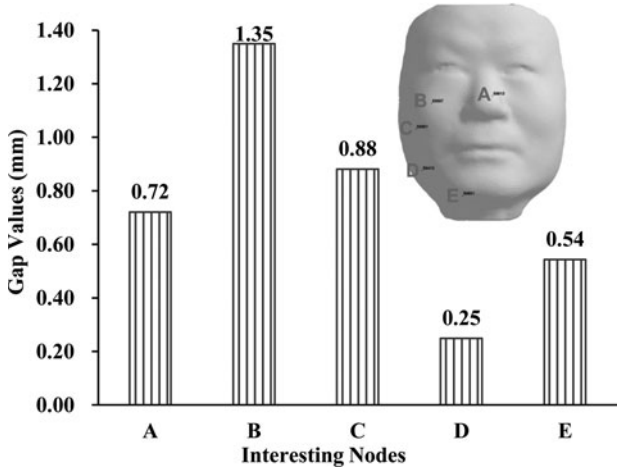

Figure 11. Five typical gaps between the headform and the respirator in a stable wearing state.

(2) including real straps in the simulation to present a real load condition,
(3) applying load forces on the nose clip after wearing the respirator,
(4) investigating effects of stiffness of the nose clip on contact characteristics,
(5) validating simulation results using contact sensors.

Conclusion

In this study, three-dimensional geometric models of a typical Chinese head and a 3M 8210 $PM_{2.5}$ respirator were developed by using CT scanning method and 3D scanning method, respectively. Corresponding FE models were generated using software HyperMesh (Altair HyperWorks, Troy, MI). Then, the wearing process of the respirator on the headform was studied by performing contact simulation using software LS-DYNA (LSTC, Livermore, CA). The wearing comfort was investigated in terms of the contact pressure and resultant deformation, and the wearing fit was investigated in terms of the relative local gap between the headform and the respirator in the steady

state. Moreover, effects of the stiffness of respirator inner layer on contact characteristics were investigated.

Simulation results show that the nasal bridge, the upper cheek, the middle cheek, the lower cheek and the chin exhibit high contact pressures while only the nasal bridge and the middle cheek have large deformations in the steady state, which means areas on the headform with high contact pressures and large deformations during the wearing process are not exactly the same. The nasal bridge exhibits the largest contact pressure up to 0.11 MPa and the middle cheek has the largest deformation of 0.93 mm. In addition, the local gap at different locations varies a lot due to the complex structure of the headform. A large gap may imply air leakage. The stiffness of respirator inner layer affects the contact pressure as well as deformation greatly.

Funding

This work was supported by the National Natural Science Foundation of China (Grant No.: 51305306), Hubei Provincial Natural Science Foundation of China (Grant No.: 2015CFB307), and the Fundamental Research Funds for the Central Universities of China (Grant No.: 2042014kf0034).

References

[1] **The World Bank**: *Cost of Pollution in China: Economic Estimates of Physical Damages*. Washington, DC: The World Bank, 2007.

[2] **WHO**: *Country Profile of Environmental Burden of Disease*: China, 2009. Available at: http://www.who.int/quantifying_ehimpacts/national/countryprofile/china.pdf.

[3] **Yu, F., G. Ma, J. Qi, and J. Wang**: *Report of China's Environmental-Economic Accounting in 2007–2008*. China Environmental Science Press, Beijing, 2012.

[4] **Chen, Z., J. Wang, G. Ma, and Y. Zhang**.: China tackles the health effects of air pollution. *Lancet 382*(9909):1959–1960 (2013).

[5] **Yang, G., Y. Wang, Y. Zeng, et al.**: Rapid health transition in China, 1990–2010: findings from the global burden of disease study. *Lancet 381*(9882):1987–2015 (2010).

[6] **Snook, S.H., W.C. Hinds, and W.A. Burgess**: Respirator comfort: subjective response to force applied to the face. *Amer. Industr. Hyg. Assoc. J. 27*(2):93–97 (1966).

[7] **Manninen, A., T. Klen, and P. Pasanen**: Evaluation of comfort and seal leakages of several respirators used in agricultural work. *Amer. Industr. Hyg. Assoc. J. 49*(6):280–285 (1988).

[8] **Akbar-Khanzadeh, F., M.S. Bisesi, and R.D. Rivas**: Comfort of personal protective equipment. *Appl. Ergon. 26*(3):195–198 (1995).

[9] **Cohen, K.S.**: Relationship of protective mask seal pressure to fit factor and head harness strap stretch. Technical Report, Army Research Laboratory, Human Engineering and Research Directorate, Adelphi, MD, 1999.

[10] **Zhuang, Z., C. Coffey, and A.R. Berry**: The effect of subject characteristics and respirator features on respirator fit. *J. Occup. Environ. Hyg. 2*(12):641–649 (2005).

[11] **Zhuang, Z., D. Groce, H.W. Ahlers, et al.**: Correlation between respirator fit and respirator fit test panel cells by respirator size. *J. Occup. Environ. Hyg. 5*(10):617–628(2008).

Bitterman, B.H.: Application of finite element modeling and analysis to the design of positive pressure oxygen masks. Master's thesis, *Air Force Institute of Technology*, Wright-Patterson Air Force Base, Ohio,1991.

[12] **Piccione, D., E.T. Moyer Jr., and K.S. Cohen**: Modeling the interface between a respirator and the human face. Human Engineering and Research Laboratory, Army Research Laboratory, Adelphi, MD, 1997.

[13] **Zhuang, Z., S. Benson, and D. Viscusi**: Digital 3-D headforms with facial features representative of the current US workforce. *Ergonomics 53*(5):661–671 (2010).

[14] **Yang, J., J. Dai, and Z. Zhang**: Simulating the interaction between a respirator and a headform using LS-DYNA. *Comput-Aid. Des. Applic. 6*(4):539–551 (2009).

[15] **Dai, J., J. Yang, and Z. Zhuang**: Sensitivity analysis of important parameters affecting contact pressure between a respirator and a headform. *Int. J. Industr. Ergon. 41*(3):268–279 (2011).

[16] **Lei, Z., J. Yang, and Z. Zhuang**: Headform and N95 filtering facepiece respirator interaction: contact pressure simulation and validation. *J. Occup. Environ. Hyg. 9*(1):46–58 (2012).

[17] **Yu, Y., S. Benson, W. Cheng, J. Hsiao, Y. Liu, Z. Zhuang, and W. Chen**: Digital 3-D headforms representative of Chinese workers. *Ann. Occup. Hyg. 56*(1):113–122 (2012).

[18] **Yang, B., K.M. Tse, N. Chen, et al.**: Development of a finite element head model for the study of impact head injury. *BioMed Res. Int.* 2014.

[19] **Drake, R.L., Vogl, A.W., and Mitchell, A.W.M.**: *Gray's Anatomy for Students*. Philadelphia: Elsevier, 2005.

[20] **Fung, Y.C.**: *Biomechanics: Mechanical Properties of Living Tissue*. 2nd ed. Springer, 1993.

[21] **Duck, F.A.**: *Physical Properties of Tissues: A Comprehensive Reference Book*. London: Academic Press, 1990.

[22] **Westreich, R.W., H.W. Courtland, P. Nasser, K. Jepsen, and W. Lawson**: Defining nasal cartilage elasticity: biomechanical testing of the tripod theory based on a cantilevered model. *Arch. Fac. Plast. Surg. 9*(4):264–270 (2007).

[23] **Lei, Z., J. Yang, Z. Zhuang, and R. Roberge**: Simulation and evaluation of respirator faceseal leaks using computational fluid dynamics and infrared imaging. *Ann. Occup. Hyg. 57*(4), 493–506 (2013).